Engineered dextranase from *Streptococcus mutans* enhances the production of longer isomaltooligosaccharides

Patcharapa Klahan, Masayuki Okuyama*, Kohei Jinnai, Min Ma, Asako Kikuchi, Yuya Kumagai, Takayoshi Tagami and Atsuo Kimura*

Research Faculty of Agriculture, Hokkaido University, Sapporo, Japan

email addresses: PK, patchakl@abs.agr.hokudai.ac.jp; MO, okuyama@abs.agr.hokudai.ac.jp; KJ, jin-chan@abs.agr.hokudai.ac.jp; MM, mamin@abs.agr.hokudai.ac.jp; AsakoK, akikuchi@abs.agr.hokudai.ac.jp; YK, ykumagai@abs.agr.hokudai.ac.jp; TT, tagami@abs.agr.hokudai.ac.jp; AtsuoK, kimura@abs.agr.hokudai.ac.jp

*Corresponding authors: Dr. Masayuki Okuyama; Kita-9 Nishi-9, Kita-ku, Sapporo 060-8589, Japan; Tel: +81-11-706-2816; email: okuyama@abs.agr.hokudai.ac.jp
Prof. Atsuo Kimura; Kita-9 Nishi-9, Kita-ku, Sapporo 060-8589, Japan; Tel/Fax: +81-11-706-2808; email: kimura@abs.agr.hokudai.ac.jp

Abbreviations: CI, cycloisomaltooligosaccharide; CITase, CI glucanotransferase; CITase-Bc, CITase from *Bacillus circulans* T-3040; DP, degree of polymerization of glucose unit; GH, glycoside hydrolase family; GTF, glucansucrase; HPAEC-PAD, high performance anion-exchange chromatography-pulsed amperometric detection; IG, isomaltooligosaccharide; IGn, IG with DP of n (n, 2–5); PNP, *p*-nitrophenol; PNP-Glc, *p*-nitrophenyl α-glucoside; PNP-IG, *p*-nitrophenyl isomaltooligosaccharide; PNP-IGn, PNP-IG with DP of n (n, 2–6); SmDex, dextranase from *Streptococcus mutans*; SmDexTM, *S. mutans* ATCC25175 SmDex bearing Gln100–Ile732

Engineered dextranase from *Streptococcus mutans* enhances the production of longer isomaltooligosaccharides

Herein, we investigated enzymatic properties and reaction specificities of *Streptococcus mutans* dextranase, which hydrolyzes α-(1→6)-glucosidic linkages in dextran to produce isomaltooligosaccharides. Reaction specificities of wild-type dextranase and its mutant derivatives were examined using dextran and a series of enzymatically prepared *p*-nitrophenyl α-isomaltooligosaccharides. In experiments with 4-mg·mL^{-1} dextran, isomaltooligosaccharides with degrees of polymerization (DP) of 3 and 4 were present at the beginning of the reaction, and glucose and isomaltose were produced by the end of the reaction. Increased concentrations of the substrate dextran (40 mg·mL^{-1}) yielded isomaltooligosaccharides with higher DP, and the mutations T558H, W279A/T563N, and W279F/T563N at the −3 and −4 subsites affected hydrolytic activities of the enzyme, likely reflecting decreases in substrate affinity at the −4 subsite. In particular, T558H increased the proportion of isomaltooligosaccharide with DP of 5 in hydrolysates following reactions with 4-mg·mL^{-1} dextran.

Key words: glycoside hydrolase family 66; dextranase; isomaltooligosaccharides; bond cleavage frequency

Introduction

Dextranase (6-α-D-glucan 6-glucanohydrolase, EC 3.2.1.11) catalyzes the endohydrolysis of α-(1→6)-glucosidic linkages in dextran. According to classifications of the glycoside hydrolase family (GH), GH49, GH31, and GH66 groups include dextranases [1]. The GH49 is a group of an inverting dextranases, whereas exo-type α-glucosidases predominate in the GH31 group and the recently discovered endo-type dextranase [2] is a unique member in this family. The GH66 group includes the dextran-active enzymes dextranase and cycloisomaltooligosaccharide glucanotransferase (CITase; (1→6)-α-D-glucan:(1→6)-α-D-glucan 6-α-D-[1→6 α-D-glucano]-transferase (cyclizing), EC 2.4.1.248), which converts dextran to cycloisomaltooligosaccharides

(CIs) using an intramolecular transglycosylation mechanism [3]. CITase was originally identified in *Bacillus* spp (currently *Bacillus circulans* T-3040), and the enzyme catalyzes the formation of cycloisomalto-heptaose (CI-7), -octaose (CI-8), and -nonaose (CI-9) [4]. Several crystal structures of GH66 enzymes have been determined previously [5–8], and $(\beta/\alpha)_8$ barrel-fold domains were identified as catalytically relevant. The characteristic architecture of CITase includes a β-jellyroll-fold domain (domain B), which is inserted at the β→α loop 7 of the catalytic domain [6,8]. This domain B was categorized as a member of the carbohydrate-binding module family 35, and was shown to recruit substrates and maintain product sizes during the formation of CIs [9]. However, this domain was not found in dextranase structures [5,7].

Streptococcus mutans (*S. mutans*) expresses glucansucrases (GTFs) that synthesize high molecular weight sticky glucans from sucrose, and these contribute to adherence of bacteria in dental caries [10,11]. Among GTFs, GTF-I, and GTF-SI are predominantly associated with the formation of insoluble glucan with α-(1→3)-glucosidic linkages, whereas GTF-S contributes to the synthesis of dextran, which is a water-soluble glucan [10]. *S. mutans* also expresses dextran degrading enzymes, an extracellular dextranase (SmDex), and an intracellular glucan α-1,6-glucosidase [12]. SmDex produces isomaltooligosaccharides (IGs) from dextran, and these are ingested by bacteria and then degraded to glucose by glucan α-1,6-glucosidase.

IGs have reported prebiotic effects [13,14], and oligosaccharides with α-(1→6)-glucosidic linkages are generally synthesized by α-glucosidase-catalyzed transglucosylation from maltooligosaccharides. However, following these reactions, some IGs include the α-(1→4)-glucosidic linkage [15], thus limiting the purity of the resulting IGs. In contrast, dextranase only produces IGs with α-1,6-glucosidic linkages. In recent years, commercial grade IGs products have become indispensable for research

in fields such as biochemistry and food science, but remain difficult to obtain. Thus, we refined the methods for producing IGs of various sizes by improving the function of SmDex with site-specific mutations. Prior to these manipulations, three-dimensional structures of GH66 [5,6] were used to predict amino acid residues that are responsible for product specificity.

As reported previously [16], we produced recombinant full-size SmDex protein in *Escherichia coli* and showed that it is subject to proteolysis, whereas N- and C-terminal truncated SmDex (SmDexTM; bearing Gln100–Ile732) proteins are not. Thus, SmDexTM was used as the parent enzyme, and patterns of hydrolytic activities were compared with those of SmDexTM derivatives by analyzing reactions with synthesized *p*-nitrophenyl isomaltooligosaccharides (PNP-IGs) and by examining carbohydrate compositions of the resulting dextran hydrolysates.

Materials and methods

Production of SmDexTM and its mutant derivatives

A pET28a-derived plasmid containing the SmDexTM coding sequence [16] was used as the template for site-directed mutagenesis, which was performed according to the PrimeSTAR Mutagenesis Basal Kit manual (Takara Bio, Shiga, Japan). Site directed mutagenesis was performed using the following oligonucleotides:

5′-GTTTGATGACCTGTTCAATCGGCAGGTTGAAACAGATGC-3′ and 5′-CAACCTGCCGATTGAACAGGTCATCAAACTTAGGAAC-3′ for MT-1; 5′-TTGATGACCTGAGCCATTCGCAGGTTGAAAC-3′ and 5′-GGCTCAGGTCATCAAACTTAGGAACATTAG-3′ for MT-2; 5′-ACCTGTTCAATTCGCAGGTTGAAACAGATGC-3′ and 5′-GCGAATTGAACAGGTCATCAAACTTAGG-3′ for MT-3; 5′-

TCAATCGGCAGGTTGAAACAGATGCTG-3′ and 5′-CAACCTGCCGATTGAACAGGTCATCAAAC for MT-4; 5′-TGGAATGCGTGGAGCCATTCGCAG-3′ and 5′-GCTCCACGCATTCCAAGACTGATCAAA-3′ for W279A; 5′-TGGAATTTGTGGAGCCATTCGCAG-3′ and 5′-GCTCCACAAATTCCAAGACTGATCAAA-3′ for W279F; 5′-CTTAGAACACGCTTATTATCCAACACAA-3′ and 5′-AATAAGCGTGTTCTAAGACACCGACACC-3′ for T558H; and 5′-TATCCAAACCAAAGCCTCAAGGTTTCG-3′ and 5′-GCTTTGGTTTGGATAATAAGCTGTTTC-3′ for T563N. Mutations were then confirmed at the DNA Sequencing Facility of the Research Faculty of Agriculture, Hokkaido University (ABI 3100 Genetic Analyzer; Applied Biosystems/Thermo, Carlsbad, CA, USA). Enzymes were produced and purified as described in our previous report [16].

Enzyme assays

Enzyme activity was measured at 35°C for 8 min using a standard reaction mixture comprising 4-mg·mL^{-1} dextran (MW of 15,000–20,000 was used throughout; Nacalai Tesque, Kyoto, Japan), 40 mM sodium acetate buffer (pH 5.0), and enzymes at appropriate concentrations. Reactions were terminated by incubating at 100°C for 10 min and reducing sugars were determined using the copper-bicinchoninate method with glucose as the standard carbohydrate. One unit of enzyme activity was defined as the amount of enzyme that produces 1 μmol of reducing sugar per min under standard conditions.

The effects of pH on rates of dextran hydrolysis were examined under standard assay conditions with the Britton-Robinson buffer at pH 2.0–10.0. The buffer contained 40 mM acetic acid, 40 mM phosphoric acid, and 40 mM boric acid, and the pH was adjusted using 0.2 M NaOH. For measurements of pH stability, SmDexTM (88 nM), W279A (91 nM), W279F (78 nM), T563N (72 nM), W279F/T563N (30 nM), W279A/T563N (46 nM), or T558H (50 nM) were incubated in Britton-Robinson buffer at 4°C for 24 h, followed by measurements of residual activity under standard assay conditions. The stable region was defined as the pH range with residual activity of > 90%. To determine thermal stability, SmDexTM (88 nM), W279A (91 nM), W279F (78 nM), T563N (72 nM), W279F/T563N (30 nM), W279A/T563N (46 nM), and T558H (50 nM) were stored in 40 mM sodium acetate buffer (pH 5.0) at 15, 20, 30, 40, 50, and 60°C for 15 min, and residual activities were then measured under standard conditions. Stable temperature regions were defined as those in which residual activity was > 90%.

The kinetic parameters k_{cat} and K_m were calculated using KaleidaGraph 3.6 J (Synergy Software, Reading, PA, USA) from a weighted Michaelis-Menten fit of initial velocities at dextran concentrations of 1.0–8.0 mg·mL^{-1} (SmDexTM), 2.0−14 mg·mL^{-1} (W279F), 2.0−12 mg·mL^{-1} (W279A), 1.0−14 mg·mL^{-1} (T563N), 1.0−35 mg·mL^{-1} (W279F/T563N), 1.0−40 mg·mL^{-1} (W279A/T563N), and 1.0−14 mg·mL^{-1} (T558H). All experiments were repeated three times and data are presented as means and standard deviations. k_{cat}/K_m values were estimated from mean values of k_{cat} and K_m, and enzyme concentrations in reaction mixtures were 88 (SmDexTM), 91 (W279A), 78 (W279F), 72 (T563N), 30 (W279F/T563N), 46 (W279A/T563N), and 50 nM (T558H).

Bond cleavage frequency analyses

To determine bond cleavage frequencies, we measured initial hydrolysis velocities of *p*-

151 nitrophenyl α-isomalto-trioside (PNP-IG3), -tetraoside (PNP-IG4), -pentaoside (PNP-
152 IG5), and -hexaoside (PNP-IG6). Reaction mixtures contained substrates at 1 mM,
153 enzymes (SmDexTM, 18, 2.5, 1.3, and 0.30 μM; W279A, 18, 9.0, 2.6, and 0.29 μM;
154 W279F, 16, 7.8, 2.0, and 0.39 μM; T558H, 10, 5.0, 1.4, and 0.42 μM; T563N, 14, 7.2,
155 1.8, and 0.29 μM; W279A/T563N, 9.3, 4.6, 1.3 and, 0.23 μM; W279F/T563N, 5.9, 3.0,
156 0.74, and 0.20 μM for PNP-IG3, -IG4, -IG5, and -IG6, respectively), and 40 mM
157 sodium acetate buffer (pH 5.0), and were incubated at 35°C. After 2 and 20 min,
158 reactions were terminated by incubating at 100°C for 10 min. The reaction products
159 were the analyzed using a Jasco HPLC system (Jasco, Tokyo, Japan) equipped with a
160 Unison UK-C18 column (ID 4.6 × 250 mm; Imtakt, Kyoto, Japan), and with an isocratic
161 mobile phase comprising 9:91 (v/v) acetonitrile:water at a flow rate of 0.5 $mL \cdot min^{-1}$ at
162 50°C. Subsequently, *p*-nitrophenyl α-glucoside (PNP-Glc) and PNP-IGs (PNP-IG2–
163 PNP-IG5) were detected at 313 nm, and their concentrations were determined from
164 peak areas using BORWIN/HSS-2000 software (Jasco). Quantitative *p*-nitrophenol
165 (PNP) release was estimated according to absorption at 400 nm in the presence of 667
166 mM sodium carbonate. PNP-IG2 was prepared as described previously [17,18]. PNP-
167 IG3, -IG4, -IG5, and -IG6 were synthesized from PNP-Glc (12 mM, Nacalai Tesque) by
168 transglucosylation of laboratory-owned oligo-1,6-glucosidase (43 nM). Products were
169 then separated by gel filtration column chromatography using a BioGel P2 column (ID
170 16 × 1,870 mm; Bio-Rad, Hercules, CA, USA) and ESI-MS spectra of purified PNP-
171 IG3–PNP-IG6 were recorded using an Exactive instrument (Thermo Fisher Scientific,
172 Waltham, MA, USA). PNP-IG3, *m/z* calculated: 624.19 $[M-H]^-$, found: 624.18; PNP-
173 IG4, *m/z* calculated: 786.24 $[M-H]^-$, found: 786.23; PNP-IG5, *m/z* calculated: 948.29
174 $[M-H]^-$, found: 948.29; PNP-IG6, *m/z* calculated: 1,110.34 $[M-H]^-$, found: 1,110.34.
175 Prior to determining hydrolytic products, isomaltohexose was prepared by partial acid

hydrolysis of dextran and was separated by gel filtration column chromatography using a BioGel P2 column.

Analysis of Dextran hydrolysates

Enzymes (780 nM) were incubated with 4-or 40-mg·mL^{-1} dextran in 40 mM sodium acetate buffer (pH 5.0) at 35°C. Reactions were terminated by incubating at 100°C for 10 min, and products were quantified using high performance anion-exchange chromatography-pulsed amperometric detection (HPAEC-PAD; Dionex ICS-3000 system; Dionex/Thermo, Idstein, Germany) with a CarboPac PA-1 column (ID 4 × 250 mm; Dionex/Thermo). Carbohydrates were separated by isocratic elution with 400 mM sodium hydroxide at a flow rate of 0.8 mL·min^{-1}.

Results and discussion

Selection of target residues for modifications of reaction specificity

The −3 and −4 subsites of SmDex were selected to transform subsite affinities and alter reaction specificities. Such transformations should yield dextran hydrolysates with differing degrees of polymerization of glucose units (DP) than that achieved using native SmDex. SmDexTM has Trp279, Trp280, Thr558, Tyr560, and Thr563 residues in the vicinity of the −3 and −4 subsites [5] (Fig. 1A). Trp279 and Trp280 are located at the β→α loop 2 of the catalytic $(\beta/\alpha)_8$ barreled domain, whereas the other three amino acids are located at the β→α loop 8. The crystal structure of CITase was used as a reference to select residues to mutate. CITase catalyzes the formation of CI-7, -8, and -9, suggesting the presence of minus subsites that can accommodate isomaltooligosyl residues with high DP. In *Bacillus circulans* T-3040 CITase (CITase-Bc), Phe207, His579, Tyr581, and Asn584 are associated with the formation of −3 and −4 subsites [6]

(Fig. 1A). Because His579 and Asn584 are part of the β→α loop 8 and correspond with Thr558 and Thr563 of SmDexTM, we generated corresponding T558H and T563N mutations. The architecture of the β→α loop 2 of CITase-Bc is distinct from the corresponding loop of SmDexTM, and is four residues longer in SmDexTM (Fig. 1A, B). Thus, the SmDexTM mutants MT-1, MT-2, MT-3, and MT-4 were generated with the CITase-like structure (Fig. 1B). MT-1 with a β→α loop 2 of the same length as CITase-Bc was generated to analyze the effects of loop lengths on specificity, and MT-2, MT-3, and MT-4 were then prepared by imposing point mutations on MT-1. However, hydrolytic activities of these proteins were below the detection limit and kinetic analyses of the contribution of the β→α loop 2 on specificity were not possible. Thus, we constructed W279A and W279F to assess the effects of the β→α loop 2 on specificity. Of the two tryptophans located within the β→α loop 2, Trp279 is unique in SmDex and in related species (Fig. 1B), and was chosen as the target residue for analyses of the influence of loop 2 divergences. In addition, the double mutants W279F/T563N and W279A/T563N were designed to investigate the effects of mutations at both the β→α loop 2 and β→α loop 8. CITase-Bc carries Phe501, Asp512, and Trp514 in domain B, and these residues are parts of subsites −3 and −4 (Fig. 1A). However, these residues were excluded from our mutation analyses because SmDexTM does not have the corresponding domain.

Production of recombinant enzymes and their characterization

The aforementioned 10 mutants were produced in *E. coli* with SmDexTM [16] as the parent enzyme. As mentioned above, hydrolytic activities of MT-1, MT-2, MT-3, and MT-4 proteins were undetectable, and specific activities of W279A and W279F were almost similar to that of SmDexTM. The specific activity of T563N was 50% less than

223 that of the parent enzyme, and other variants showed activity decreases between 8% and
224 20% (Table 1). No mutant enzymes produced detectable amounts of CI. The optimal pH
225 for SmDexTM and its derivatives was 5.0, whereas that for T558H was 4.2. These
226 mutations showed minimal influences on pH stability ranges when compared with that
227 of the parent enzyme, and thermal stabilities of the mutants were almost identical to that
228 of SmDexTM (Table 1).

229 Table 2 summarizes the kinetic parameters for hydrolysis of dextran by
230 SmDexTM and the present mutants. Hydrolytic rates in the presence of various dextran
231 concentrations followed Michaelis-Menten relationships, and K_m values were greater for
232 all mutants than for SmDexTM, and remarkable increases were observed for the double
233 mutants W279A/T563N and W279F/T563N. Double replacements at Trp279 and
234 Thr563 affected the formation of the ES complex, although k_{cat} values of most of these
235 mutants varied between 65% and 145% of parent protein values. Only the mutant
236 T558H gave a much lower value (41%) when compared with the parent protein, and the
237 mutation to Thr558 likely affected the reactivity of the ES complex and/or the product
238 release step from the EP complex.

239 Hydrolytic products of SmDexTM with 1 mM isomaltohexaose (IG6) were
240 monitored using HPAEC-PAD, and productions of glucose, isomaltose (IG2), isomalto-
241 triose (IG3) -tetraose (IG4), and -pentaose (IG5) were observed. Production rates of
242 glucose, IG2, and IG3 were 1.61 ± 0.15, 1.52 ± 0.05, and 0.548 ± 0.041 μmol/min/mg
243 protein, respectively. Because two moles of IG3 are produced from one mole of IG6,
244 the calculated intrinsic rate of IG3 production is 0.274 μmol/min/mg. Except for the
245 reaction that generate IG3, IG6 has two binding modes and these were indistinguishable
246 in these experiments (Fig. 2A). Accordingly, our analyses give limited information
247 about hydrolytic patterns of SmDexTM in the presence of IG6. Further experiments

using [^{14}C]glucose labeled IGs may reveal their binding modes, as shown in a reported [19] analysis of action patterns and subsite maps of *S. mutans* KI-R dextranase.

Analysis of bond cleavage frequencies by SmDexTM and its mutants using PNP-IGs

In this study, we developed a method for estimating binding modes of substrate to SmDexTM using a series of PNP-IGs instead of radioactive substrate. PNP-IGs readily enabled the identification of cleavage sites and quantification of their hydrolytic products with the chromogenic PNP group using a RP-HPLC–UV detector. Thus, a series of PNP-IGs were enzymatically prepared and initial rates of SmDexTM mediated hydrolysis of 1 mM PNP-IG3–PNP-IG6 were determined (Fig. 2B). The enzyme hydrolyzed all PNP-IGs except PNP-IG3, and the highest hydrolytic rate of SmDexTM was achieved with PNP-IG6. In addition, the enzyme produced only PNP-Glc from PNP-IG4, and preferentially released PNP-Glc with small amounts of PNP-IG3 from PNP-IG5 or PNP-IG6. SmDexTM did not yield detectable amounts of PNP or PNP-IG2 in catalysis of any of the present PNP-IGs substrates.

Binding of PNP to subsites may influence functional evaluations of PNP-IGs in analyses of hydrolytic patterns of SmDexTM, because PNP is a mimic of glucosyl moieties. The failure of PNP production from PNP-IG5, however, disagrees with production of glucose from IG6 (Fig. 2A), indicating that SmDexTM cannot hydrolyze the heteroside linkage between α-glucoside and PNP. In contrast, other enzymes with specificity toward α-(1→6)-glucosidic linkages, such as glucan α-1,6-glucosidase and oligo-1,6-glucosidase, can hydrolyze these heteroside linkages [17, 20]. However, SmDex likely has a more rigid +1 subsite than those of α-(1→6)-specific enzymes, and hence, exhibits strict specificity toward the α-(1→6)-glucosidic linkage. Moreover, the lack of PNP-IG2 production from PNP-IG5 reflects lower production of IG3, rather

than low production of glucose and IG2 from IG6 (Fig. 2A). Additionally, the +3 subsite may not be suitable for PNP, because PNP-IG2 was not produced from any other PNP-IGs. Three-dimensional structures of SmDex with bound ligands to plus subsites are not available and the details of substrate binding to plus subsites remain unknown. However, Trp455 and Phe457 are expected to be located at plus subsites [5], and interactions, such as π-π interactions, of their side chains with PNP may facilitate binding of PNP to plus subsites other than the +3 subsite.

As with SmDexTM, all mutant enzymes exhibited higher hydrolytic rates toward PNP-IG6 than toward PNP-IG5 and PNP-IG4, and no activity toward PNP-IG3 (Fig. 3). The hydrolytic pattern of W279A was similar to that of SmDexTM, whereas those of W279F, T563N, W279F/T563N, W279A/T563N, and T558H were altered (Fig. 3). In these variants, proportions of released PNP-Glc were decreased following hydrolysis of PNP-IG5 and PNP-IG6. In particular, significant decreases in the proportion of PNP-Glc was noted in W279F/T563N, W279A/T563N, and T558H when PNP-IG6 was used as the substrate (Fig. 3). In these three mutants, percentage velocities of PNP-Glc were less than that of PNP-IG3, and it is assumed that these mutations decreased the affinity at the −4 subsite, leading to changes in the binding mode of PNP-IG6. Alternatively, we suggest that reduced affinity at the −5 subsite may also change the hydrolytic action patterns. However, during hydrolysis of PNP-IG5, decreased affinity at the −5 subsite is unlikely to increase the proportion of released PNP-IG3, suggesting that the decrease in −4 subsite affinity reflects changes in the binding modes of PNP-IG5 and PNP-IG6.

Mutation related changes in hydrolysis rates with the present PNP-IGs were smaller than those with dextran (Table 1), suggesting that the decreases in observed hydrolytic rates are related to the size of the substrate. During hydrolysis of dextran, all

298 subsites are occupied by the substrate, and mutations of subsites measurably influenced
299 the hydrolysis of dextran. In contrast, subsite-binding modes of PNP-IGs can be
300 changed by selecting a high affinity-binding mode, which only leads to small decreases
301 in reaction rates of mutants. To evaluate the effects of changes in subsite affinities, we
302 should determine kinetic parameters for hydrolysis of PNP-IGs as well as dextran.
303 However, it was difficult to determine K_m values for the series of PNP-IGs, because rate
304 estimates were hampered by multiple degradation modes.
305 Herein, we formed PNP conjugates to facilitate detection of hydrolytic products,
306 but found that these influenced PNP-IG binding to plus subsites. However, reductions in
307 affinities of PNP-IGs for mutant minus subsites could be detected, indicating that PNP-
308 IGs are suitable for assessments of minus subsites of dextranases, including SmDex.

309 ***Analysis of dextran hydrolysates in reactions of SmDexTM and its mutants***

310 Dextran (4 or 40 mg·mL^{-1}) was hydrolyzed by SmDexTM, and the resulting
311 carbohydrate compositions in 2, 8, and 24-h reaction mixtures were analyzed using
312 HPAEC-PAD. With an initial dextran concentration of 4 mg·mL^{-1}, the 2-h reaction
313 mixture with SmDexTM predominantly contained IG2, IG3, and IG4, with trace
314 concentrations of IG5 (Fig. 4A). Following longer reaction times, percentage of glucose
315 and IG2 contents of reaction mixtures increased, whereas those of IG3 and IG4
316 decreased. In the 24-h reaction mixture, 83% of the dextran had been converted,
317 predominantly to glucose and IG2, and increases in mono- and disaccharide
318 concentrations followed further hydrolysis of the intermediates IG3, IG4, and IG5.
319 Bond cleavage frequency analyses demonstrated that SmDexTM failed to hydrolyze
320 PNP-IG3, but hydrolyzed IG3 into glucose and IG2. In subsequent experiments,
321 increased initial dextran concentrations of 40 mg·mL^{-1} led to lower concentration ratios

of glucose and increased ratios of IG5, which was degraded with longer reaction times (Fig. 4B). In these reactions, 83% of dextran was consumed after 24 h incubation and ratios of IG3 and IG4 were higher than in reactions containing 4 $mg \cdot mL^{-1}$ dextran. Therefore, high dextran concentrations are suitable for obtaining IGs with high DP using SmDexTM.

To examine dextran hydrolysis by the present mutants, we determined hydrolysate concentrations after reactions. The effects of the present mutations were prominent at a dextran concentration of 4 $mg \cdot mL^{-1}$ (Fig. 4A), and ratios of IGs were higher following reactions with mutants than with SmDexTM. In W274A/F, almost half of the products were IG2 and IG3 in 24-h reactions, and about 80% of the dextran was degraded. In contrast, negligible amounts of IG3 remained following reactions with the parent enzyme, and 24-h reaction mixtures of W274F/T563N and W274A/T563N had carbohydrate compositions similar to those of W274A/F, whereas that of T563N was similar to hydrolysates from SmDexTM reactions. These data indicate that the Trp279 mutation strongly influences the characteristics of double mutant enzymes. T558H showed a carbohydrate composition that was distinctly different from the parent enzyme. Specifically, almost 50% of the dextran in the reaction mixture was degraded after 2 h, and high proportions of IGs were observed, predominantly IG5. In addition, IG4 remain in the reaction mixture at 24 h, suggesting that decreased affinity at the −4 subsite due to the substitution of His for Thr588 reduces the enzyme-substrate binding energy during the hydrolysis of IG4 and IG5, and leads to reduced hydrolytic activities and decreased IG consumption ratios. At a substrate concentration of 40 $mg \cdot mL^{-1}$, carbohydrate profiles following reactions of mutant enzymes differed little from that of SmDexTM (Fig. 4B). In all cases, glucose and IG2–IG5 were detected during the early stages of the reaction, and IGs with high DP decreased over time. Following 24-h

reactions of T563N, T558H, W279A/T563N, and W279F/T563H, ratios of IGs contents were slightly higher and glucose concentrations were lower than those of the parent enzyme.

Pronounced effects of mutations on hydrolysates at the lower concentration of dextran (4 $mg \cdot mL^{-1}$) likely correspond with differences in IGs concentrations in the reaction mixture. Ratios of IGs to dextran concentrations increased more rapidly at the lower dextran concentration than at the higher dextran concentration (40 $mg \cdot mL^{-1}$). At the high dextran concentration, enzyme reactions with IGs substrates are much less likely, because dextran, which is the preferred substrate, remained in the reaction solutions for longer period. As seen in hydrolysis experiments with PNP-IGs (Fig. 3), the mutations can influence hydrolytic patterns toward IGs. Consequently, the effects of mutations were more marked at the lower dextran concentration.

In summary, we generated several mutant enzymes according to structural comparisons with CITase and evaluated their hydrolytic activities toward PNP-IGs and dextran. These experiments showed that the binding mode of PNP-IG5 and -IG6 changed in W279F/T563N, W279A/T563N, and T558H mutant enzymes, due to decreased affinities at the −4 subsite. We also showed that all variants, except for T563N, generated IGs with higher DP than SmDexTM in the presence of low concentrations of dextran. Finally, T558H achieved a high proportion of IG5 in reaction mixtures (Fig. 4), and is therefore a promising candidate for the production of IGs with high DP from dextran.

Author contributions

K.P. conducted most of the experiments and analyzed the results with help from M.O., T.T. and Atsuo K. M.M., Y.K., and Asako K. were involved in analytical HPLC and HPAEC-PAD analyses. K.J. contributed to the preparation of IG6. M.O. and Atsuo K. conceived the project

and wrote the paper with K.P. All authors have reviewed the results and approved the final version of the manuscript.

Disclosure statement

No potential conflict of interest was reported by the authors.

Acknowledgements

We thank the staff of the Instrumental Analysis Division of the Creative Research Institution at Hokkaido University for amino acid and mass spectrometric analyses. The authors would like to thank Enago (www.enago.jp) for the English language review.

References

[1] Lombard V, Golaconda Ramulu H, Drula E, et al. The carbohydrate-active enzymes database (CAZy) in 2013. Nucleic Acids Res. 2014;42:D490–D495.

[2] Gozu Y, Ishizaki Y, Hosoyama Y, et al. A glycoside hydrolase family 31 dextranase with high transglucosylation activity from Flavobacterium johnsoniae. Biosci. Biotechnol. Biochem. 2016;80:1562–1567.

[3] Oguma T, Tobe K, Kobayashi M. Purification and properties of a novel enzyme from Bacillus spp. T-3040, which catalyzes the conversion of dextran to cyclic isomaltooligosaccharides. FEBS lett. 1994;345:135–138.

[4] Oguma T, Horiuchi T, Kobayashi M. Novel Cyclic Dextrins, Cycloisomaltooligosaccharides, from Bacillus sp. T-3040 Culture. Biosci. Biotechnol. Biochem. 1993;57:1225–1227.

[5] Suzuki N, Kim YM, Fujimoto Z, et al. Structural elucidation of dextran degradation mechanism by Streptococcus mutans dextranase belonging to glycoside hydrolase family 66. J. Biol. Chem. 2012;287:19916–19926.

[6] Suzuki N, Fujimoto Z, Kim YM, et al. Structural elucidation of the cyclization mechanism of α-1,6-glucan by Bacillus circulans T-3040 cycloisomaltooligosaccharide glucanotransferase. J. Biol. Chem. 2014;289:12040–12051.

[7] Suzuki N, Kishine N, Fujimoto Z, et al. Crystal structure of thermophilic dextranase from Thermoanaerobacter pseudethanolicus. J. Biochem. 2015;159:331–339.

[8] Fujimoto Z, Kishine N, Suzuki N, et al. Isomaltooligosaccharide-binding structure of Paenibacillussp. 598K cycloisomaltooligosaccharide glucanotransferase. Biosci. Rep. 2017;37:BSR20170253.

[9] Suzuki R, Suzuki N, Fujimoto Z, et al. Molecular engineering of cycloisomaltooligosaccharide glucanotransferase from Bacillus circulans T-3040: structural determinants for the reaction product size and reactivity. Biochem. J. 2015;467:259–270.

[10] Monchois V, Willemot RM, Monsan P. Glucansucrases: mechanism of action and structure–function relationships. FEMS Microbiol. Rev. 1999;23:131–151.

[11] Tamesada M, Kawabata S, Fujiwara T, et al. Synergistic effects of Streptococcal glucosyltransferases on adhesive biofilm formation. J. Dent. Res. 2004;83:874–879.

[12] Colby SM, Whiting GC, Tao L, et al. Insertional inactivation of the Streptococcus mutans dexA (dextranase) gene results in altered adherence and dextran catabolism. Microbiology (Reading, Engl.) 1995;141:2929–2936.

[13] Kohmoto T, Fukui F, Takaku H, et al. Effect of isomalto-oligosaccharides on human fecal flora. Bifidobacteria and microflora. 1988;7:61–69.

[14] Kohmoto T, Fukui F, Takaku H, et al. Dose-response test of isomaltooligosaccharides for increasing fecal bifidobacteria. Agric. Biol. Chem. 1991;55:2157–2159.

[15] Ma M, Okuyama M, Sato M, et al. Effects of mutation of Asn694 in Aspergillus niger α-glucosidase on hydrolysis and transglucosylation. Appl. Microbiol. Biotechnol. 2017;101:6399–6408.

[16] Kim YM, Shimizu R, Nakai H, et al. Truncation of N- and C-terminal regions of Streptococcus mutans dextranase enhances catalytic activity. Appl. Microbiol. Biotechnol. 2011;91:329–339.

[17] Saburi W, Mori H, Saito S, et al. Structural elements in dextran glucosidase responsible for high specificity to long chain substrate. Biochim. Biophys. Acta 2006;1764:688–698.

[18] Kobayashi M, Saburi W, Nakatsuka D, et al. Structural insights into the catalytic reaction that is involved in the reorientation of Trp238 at the substrate-binding site in GH13 dextran glucosidase. FEBS Lett. 2015;589:484–489.

[19] Pulkownik A, Thoma JA, Walker GJ. The action pattern and subsite map of Streptococcus mutans K1-R dextranase. Carbohydr. Res. 1978;61:493–497.

[20] Okuyama M, Saburi W, Mori H, et al. α-Glucosidases and α-1,4-glucan lyases: structures, functions, and physiological actions. Cell Mol Life Sci. 2016;73:2727–2751.

[21] Davies G, Wilson K, Henrissat B. Nomenclature for sugar-binding subsites in glycosyl hydrolases. Biochem. J. 1997;321:557–559.

446 Table 1. Basic properties of SmDexTM and its mutant derivatives

Enzyme	Specific activity (U/mg)	Optimum pH	pH stability [a]	Thermal stability (°C) [a]
SmDexTM	58	5.0	4.0 – 9.0	< 40
W279A	43	5.0	4.0 – 10.0	< 40
W279F	46	5.0	3.0 – 10.0	< 40
T558H	11	4.2	3.5 – 8.0	< 40
T563N	27	5.0	4.0 – 9.0	< 40
W279A/T563N	6.1	5.0	4.0 – 8.0	< 40
W279F/T563N	4.7	5.0	4.0 – 8.0	< 38

447 [a] Range at which residual activity is more than 90%

448 Table 2. Kinetic parameters of SmDexTM and its mutant derivatives for the hydrolysis
449 of dextran

Enzyme	K_m (mg·mL^{-1})	k_{cat} (s^{-1})	k_{cat}/K_m (s^{-1}·mL·mg^{-1})
SmDexTM	1.8 ± 0.1	77 ± 1	43
W279A	6.1 ± 0.1	99 ± 1	16
W279F	5.4 ± 0.1	110 ± 0	20
T558H	4.2 ± 0.1	29 ± 1	6.9
T563N	5.2 ± 0.5	57 ± 1	11
W279A/T563N	61 ± 1	98 ± 1	1.6
W279F/T563N	32 ± 1	50 ± 1	1.6

450 k_{cat} and K_m values are presented as means ± standard deviation of triplicate
451 measurements.

Figure captions

Fig. 1. Three-dimensional structure comparisons of SmDexTM (PDB ID: 3VMN; *green*) and CITase-Bc (PDB ID: 3WNL; *yellow*; A) and multiple sequence alignment of a part of the β→α loop 2 of the catalytic $(\beta/\alpha)_8$ barrel of GH66 enzymes (B)

(A) Depicted residues are associated with the formation of −3 and −4 subsites. Numbers in italics represent residues of CITase-Bc. (B) Characters on the left side indicate UniProtKB accession numbers or enzymes (Smdex, MT-1–MT-4, and CITase-BC). Multiple sequence alignments were performed using MAFFTash (https://sysimm.ifrec.osaka-u.ac.jp/MAFFTash/).

Fig. 2. Schematics of IG6, PNP-IG4, -IG5, and -IG6 binding subsites in SmDexTM

Circles are glucose residues and lines between two circles show α-(1→6)-glucosidic linkages. The subsite number notation is in accordance with the system using "–*n*" and "+*n*" [21]. (A) The values on the right indicate release rates of glucose (binding modes 1 and 2), IG2 (binding modes 3 and 4), and IG3 (binding mode 5). (B) The values on the right side represent release rates of either PNP-Glc or PNP-IG3. Numbers in parentheses are bond cleavage frequencies.

Fig. 3. Bond cleavage frequency of PNP-IG4–PNP-IG6 by SmDexTM and its variants

The values on the right side indicate reaction rates. The numbers above the substrates indicate bond cleavage frequencies.

Fig. 4. Percentage compositions of products in dextran hydrolysates

Glucose (*white*), IG2 (*light gray*), IG3 (*dark gray*), IG4 (*black*), and IG5 (*dot*) at 2, 8, and 24 h; (A) $[\text{dextran}]_0 = 4\ \text{mg}\cdot\text{mL}^{-1}$; (B) $[\text{dextran}]_0 = 40\ \text{mg}\cdot\text{mL}^{-1}$.

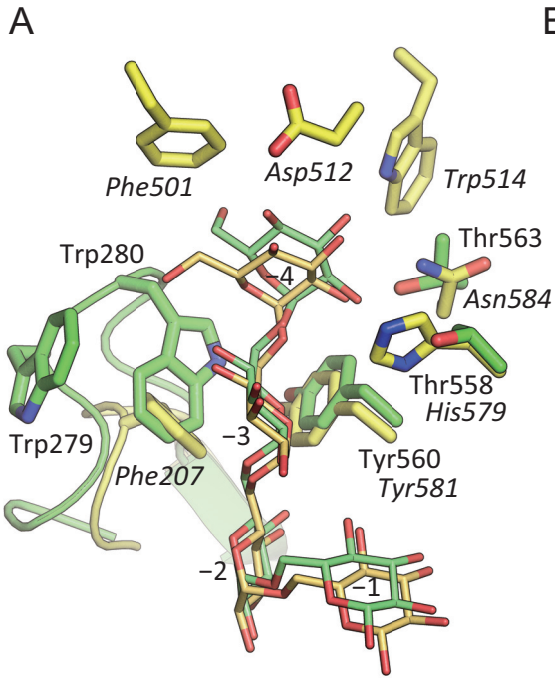

B

```
                279
                ▼
SmDex  : QSWNWWSHSQVE
Q54443 : QSWNWWSHSQVE
Q76EQ4 : QSWNWWSHSKVE
A4F2S5 : QDWNTWSGSEID
Q1MVS0 : QDWNTWSGSEID
Q8VLP4 : QDWNTWSGSEID
P39653 : QDWNTWSGSEID
Q59979 : QKWNTWSHTQVD
  MT-1 : Q-WS---HSQVE
  MT-2 : D-LS---HSQVE
  MT-3 : D-LF---NSQVE
  MT-4 : D-LF---NRQVE
CITase-Bc : D-LF---NREIS
P70873 : D-LF---NRQIS
G9MBW2 : D-LF---NREIS
Q8A368 : D-IA---NRPVH
Q6VUH2 : D-IA---NRPVA
Q6VUG9 : D-IA---NRQVS
Q6VUG7 : D-IA---NREVS
B0KBZ7 : D-IA---NRDIY
Q6VUH6 : D-WS---GRMIY
Q6VUH4 : D-WS---GRPIY
H2EI27 : D-LL---GRTLY
A8F6K5 : D--AWWRKRYIS
```

Figure 1. Klahan et al

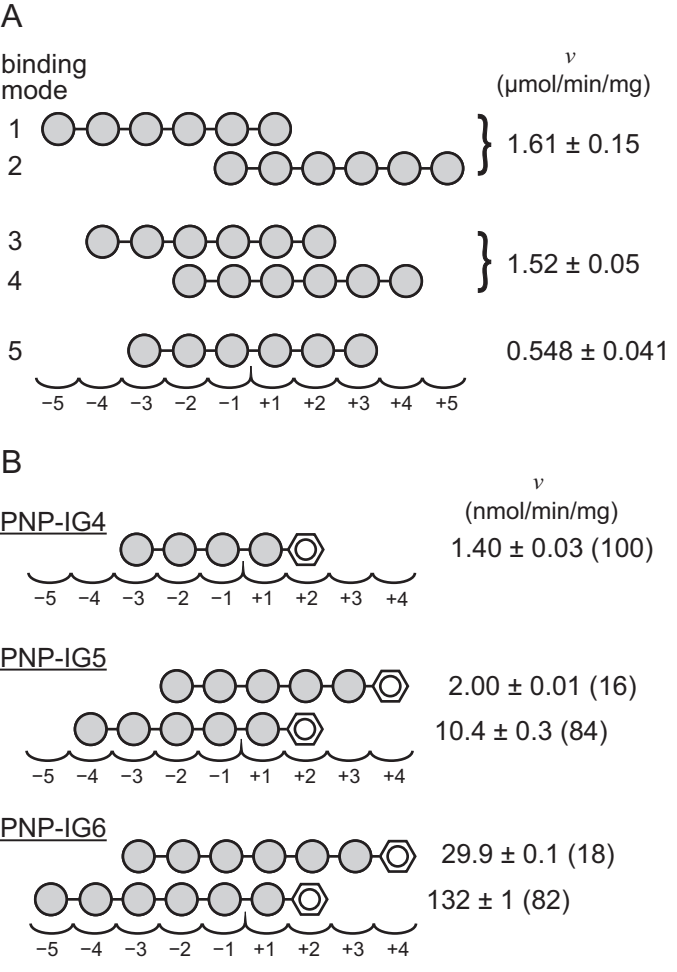

Figure 2. Klahan et al

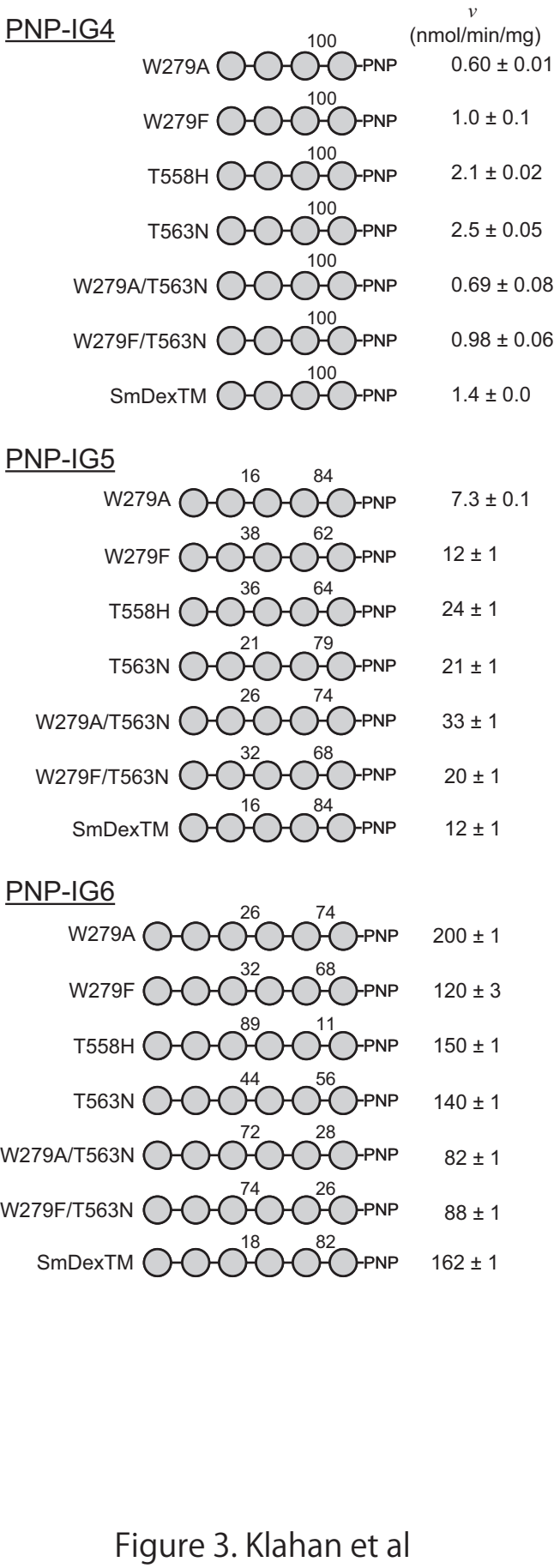

Figure 3. Klahan et al

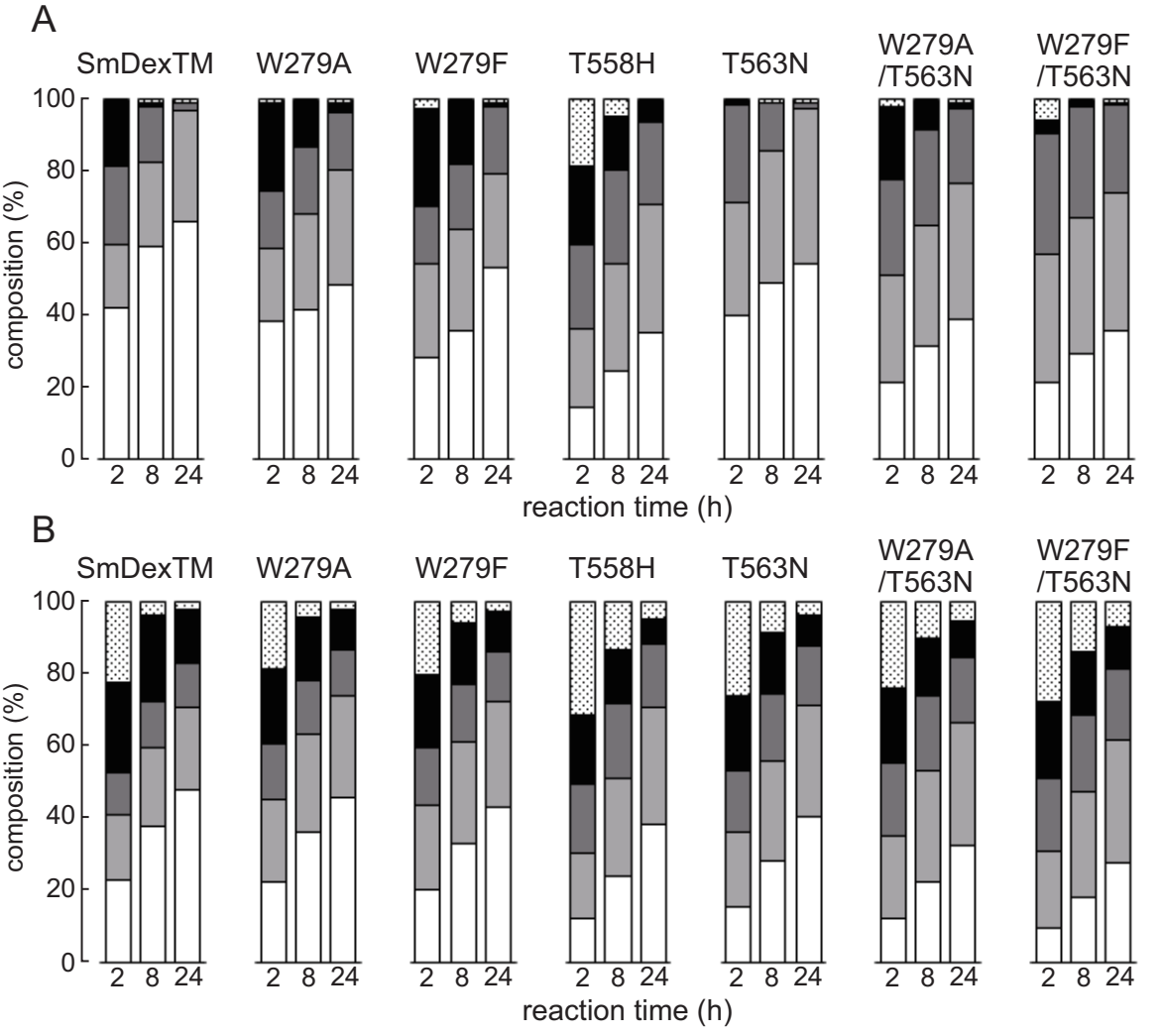

Figure 4. Klahan et al